Analyzing Power Beacon Assisted Multi-Source Transmission Using Markov Chain

Xuanxuan Tang, Yansha Deng, *Member, IEEE*, Yueming Cai, *Senior Member, IEEE*, Wendong Yang, and Arumugam Nallanathan, *Fellow, IEEE*

Abstract—**Wireless power transmission (WPT) is envisioned to be a promising technology for prolonging the lifetime of wireless devices in energy-constrained networks. This paper presents a general power beacon (PB) assisted multi-source transmission, where a practical source selection scheme with information transmission (IT) mode or non-IT mode is developed to maximize the transmission reliability. In the IT mode, a zero-forcing (ZF) beamformed signal with no interference to the destination is transmitted at the multi-antenna PB to supply wireless energy for the sources, and bring non-negative effect to the destination. Among multiple sources, the energy-sufficient source with the best channel quality is selected for wireless information transmission (WIT), while the other sources remain for energy harvesting. In the non-IT mode, the equal power transmission is adopted at PB to focus on energy delivery. Using Markov chain theory, the energy arrival and departure of each finite-capacity storage at the source is characterized mathematically, and the comprehensive analytical expressions of the energy outage probability (EOP), the connection outage probability (COP), and the average transmission delay (ATD) are formulated and derived. Our results reveal that the EOP, COP, and ATD can be significantly improved via increasing the number of sources deployed in the proposed network with finite transmit power of PB. We also prove that the multi-source network will never experience energy outage with infinite transmit power of PB.**

Index Terms—**Wireless power transfer, Markov chain, energy storage, energy outage probability, average transmission delay.**

I. INTRODUCTION

The lifetime of current wireless devices is significantly limited by the energy capacity of their batteries, especially in some energy-constrained scenarios, such as wireless sensor networks (WSNs) [1], wireless body area networks (WBANs) [2], and low-power wide-area networks (LPWANs) [3]. To cope with this limitation, the energy harvesting (EH) has emerged as a promising technology to enable the sustainable energy for the devices without replacing their battery [4, 5]. Harvesting energy from the ambient environment sources like solar, wind, thermoelectric, electromechanical, etc, has

been extensively researched and applied in industry. However, this approach does not suitable for wireless communication devices, as it could not guarantee controllable and continuous energy supply due to the randomness and instability of the environment, which may degrade the user experience.

Recently, the wireless power transmission (WPT) via radio-frequency (RF) radiation has drawn much attention among the wireless communities due to the great advancements of microwave technologies over the past decades [6, 7]. Compared with collecting energy via natural sources, WPT is capable of delivering a controllable amount of energy as well as information. In order to realize WPT in practice, the simultaneous wireless information and power transmission (SWIPT) via the same modulated microwave has been proposed and discussed extensively in existing literature. Specifically, two classic practical architectures have been presented, namely the "time-switching" architecture [8, 9] and the "power-splitting" architecture [10–12], where the receiving signal can be splitted either over time or power domain for independent WPT and wireless information transmission (WIT), respectively. Note that the efficiency of WPT relies on the received signal power while the reliability of WIT hinges on the received signal-to-noise ratio (SNR) [13], as the noise power is relatively low, the distance for WPT is drastically shorter than that for WIT. Under this circumstance, the short range limitation of WPT and the same propagation link between WPT and WIT largely limit the information transmission range.

To face the challenge of aforementioned SWIPT design, some works have proposed the power beacon (PB) assisted WPT systems [13, 14]. In such systems, WPT and WIT processes are decoupled and the PB can be deployed much closer to the wireless-powered equipments, which boosts the efficiency of WPT significantly. In 2017, the PB-based product "Cota Tile" has been designed by Ossia Inc. to charge wireless devices at home, which has received the "Innovation Awards" at the 2017 Consumer Electronics Show (CES) [15]. In [16], a novel PB assisted wiretap channel was studied to exploit secure communication between the energy constrained source and a legitimate user under eavesdropping. In [17], the authors studied a PB assisted wireless-powered system, where each user first harvested energy from RF signals broadcast by its associated access point (AP) and/or the PB in the downlink and then used the harvested energy for information transmission in the uplink. The fraction of the time duration for downlink WPT was then optimized for each user. In [18], the users clustering around the PB for WPT, and deliver information to the APs. In [19], the device-to-device (D2D) communication sharing the

resources of downlink cellular network was powered by the energy from PBs.

The aforementioned works have assumed no energy storage across different time slots, and the wireless-powered devices consume all the harvested energy in the current time slot to perform its own information transmission (IT). This type of operating mode, named as "harvest-use" [20], may not practical due to the following two-fold reasons: 1) the wireless devices are usually equipped with battery, which can store energy over different time slots; and 2) the "harvest-use" approach results in the random fluctuation of the instant transmit power of a wireless-powered device, which may not only affect the performance of the device itself, but also create chaos to the whole system.

Recent research have shifted to the so-called "harvest-store-use" operating mode [21], where the devices are capable of storing the harvested energy in a rechargeable battery. In [22], an accumulate-and-jam protocol was presented to enhance the physical layer security in wireless transmission. The full-duplex (FD) relaying scheme was studied in the WPT networks in [23, 24]. Unlike the single energy storage scenario in [22–24], the multiple energy storages were considered in [25] and [26] with energy harvested from natural sources and wireless signals, respectively. In [26], a wireless-powered uplink and downlink network was studied, where the WPT occurs in the downlink performing by time division AP, and the IT occurs in both uplink and downlink, where the AP transmits the downlink information, and the users use the harvested energy storing for uplink information. Both the energy at the AP and the users are modelled using Markov chain, and the time-frequency resource allocation and user scheduling problem was studied to minimize overall energy consumption.

In this paper, we study the energy storage and data transmission of PB assisted wireless-powered multi-source networks, where the network can operate in the non-IT mode or the IT mode. In the non-IT without any energy sufficient sources, the whole network experiences energy outage event with no IT in the network, thus the PB uses the equal power allocation among all antennas for directing its energy. In the IT mode, the source with the best channel quality among all the energy-sufficient sources is selected for IT, to avoid the interference from the PB to the destination, a zero-forcing (ZF) beamformed signal is designed during the WPT, with no inteference to the data transmission between the source and the destination.

- We formulate a Markov-based analytical framework for the energy storage and energy usage of the proposed multi-source wireless-powered networks to characterize its dynamic behaviors of the energy arrival and departure. To facilitate the network performance analysis, we also derive the state transition probabilities of the proposed network, and the stationary probabilities of all the states.
- We propose a operating mode selection procedure for the proposed network to select the non-IT mode and the IT mode based on the energy states of all the sources. A flexible beamforming transmission scheme is proposed at the PB, which can adapt to the network operating mode. In the non-IT mode, the beamformer is designed

with equal power among antennas. In the IT mode, the beamformer is designed to bring no interference to the data transmission between the selected source and the destination.

- Based on our derived stationary probabilities of all the states, we derive the energy outage probability (EOP) and the connection outage probability (COP) of proposed network in the non-IT mode and the IT mode, respectively. To quantify the delay performance, we also define and derive analytical expression for the average transmission delay (ATD) of proposed networks. Our derived analytical results are all validated via simulation, which show the correctness of our derivations, and demonstrate design insights.

The remainder of the work is organized as follows: Section II describes the system model and presents the details of the operating mode selection as well as the source selection procedure. In III, the energy state transitions among all the states are carried out. In IV, the energy outage probability, the connection outage probability, and the average transmission delay of the network are respectively investigated. Simulation results are given in Section V, and Section VI summarizes the contributions of this paper.

Notation: Throughout this paper, the boldface uppercase letters are used to denote matrices or vectors. $(\cdot)^T$, $(\cdot)^H$, and $(\cdot)^\dagger$ are denoted as the transpose operation, the conjugate transpose operation, and the orthogonal operation, respectively. $F_\gamma(\cdot)$ and $f_\gamma(\cdot)$ represent the cumulative distribution function (CDF) and the probability density function (PDF) of random variable γ, respectively. $\mathbb{E}[\cdot]$ denotes the expectation operation. $\exists$, $\forall$, and $\exists!$ stand for the existential quantifier, the universal quantifier, and the unique existential quantifier, respectively. A list of the fundamental variables is provided in Table I.

II. SYSTEM MODEL

We consider a multi-source wireless-powered transmission network as shown in Fig. 1, which consists of single PB node B, K number of wireless-powered source nodes $\{S_k\}_{k=1}^K$, and a destination node D. It is assumed that B is equipped with N_B antennas, and all the other nodes are equipped with a single antenna, where all nodes are working in half-duplex (HD) mode. Each source (IoT/ mobile device) is equipped with an energy storage with a finite energy capacity of ε_T. We assume that all the channels experience quasi-static Rayleigh fading and the channel coefficients keep constant during a block time T_0 but change independently from one packet time to another[1]. A standard path-loss model [8, 29] is adopted, namely the average channel power gain $\bar{\gamma}_{ab} = \mathbb{E}\left[|h_{ab}|^2\right] = d_{ab}^{-\alpha}$, where α is the path-loss factor, h_{ab} and d_{ab} denote the channel coefficient and the distance between a and b, respectively.

A. Energy Discretization and State Modeling

To quantify the energy storage at the sources, we define a discrete-level model [22, 24], namely, each storage is discretized into $1 + L$ levels, where L is the discretizing level of

[1]This assumption has been extensively adopted in the WPT researches [22, 27, 28].

TABLE I
LIST OF FUNDAMENTAL VARIABLES

| Symbol	Description
K	Number of sources
N_B	Number of antennas at the power beacon
ε_T	Energy capacity of the energy storage at each source
T_0	Block time duration
h_{ab}	Channel coefficient between a and b
$\mathbf{h}_{ab}$	Channel coefficient vector between a and b
d_{ab}	Distance between a and b
$\bar{\gamma}_{ab}$	Average channel power gain between a and b
α	Path-loss factor
ε_l	Energy of the lth energy level
ε_Δ	Single unit of energy
$\vec{s}_n, \vec{s}_{n'}$	The nth and n'th energy state, respectively
l_k^n	Energy level of the kth source at state $\vec{s}_n$
Θ	Set of all the energy states
Θ_1	Set of energy states in non-IT operating mode
Θ_2	Set of energy states in IT operating mode
N	Number of energy states in Θ
N_1	Number of energy states in Θ_1
N_2	Number of energy states in Θ_2
C_0	A constant properly set for the operating mode selection
ϑ_n^{TH}	Set of indexes of source nodes that are in IT operating mode at state $\vec{s}_n$
l_S^{th}	Transmit energy level threshold of sources
ε_S^{th}	Transmit energy threshold of sources
K_n^{TH}	Number of elements in ϑ_n^{TH}
Φ_0	Empty set
η	Energy conversion efficiency
P_B	Transmit power of the power beacon
$\mathbf{w}_1$	Normalized weight vector applied at the power beacon in non-IT operating mode
$\mathbf{w}_2$	Normalized weight vector applied at the power beacon in IT operating mode
N_0	Power density of the AWGN
P_S	Transmit power of sources
l_S	Actual transmit energy level of sources
$\Delta \vec{s}_n$	Energy level increment vector from $\vec{s}_n$ to $\vec{s}_{n'}$
Δl_k^n	Energy level increment of S_k from $\vec{s}_n$ to $\vec{s}_{n'}$
$\Theta_1^{n,n'}$	Set of all qualified $\vec{s}_{n'}$, which is the subset of Θ and its construction relies on the specific $\vec{s}_n$
$\Theta_2^{n,n',i*}$	Set of all qualified $\vec{s}_{n'}$, which is the subset of Θ and its construction relies on the specific $\vec{s}_n$ and the value of $i*$
$p_k^{n \to n'}$	Transition probability of S_k to transfer from l_k^n to $l_k^{n'}$ within one step in non-IT operating mode
$p_{\vec{s}_n \to \vec{s}_{n'}}^1$	Transition probability to transfer from $\vec{s}_n$ to $\vec{s}_{n'}$ within one step in non-IT operating mode
$p_k^{n \to n',i}$	Transition probability of S_k to transfer from l_k^n to $l_k^{n'}$ within one step in IT operating mode when S_{i*} is selected
$p_{\vec{s}_n \to \vec{s}_{n'}}^2$	Transition probability to transfer from $\vec{s}_n$ to $\vec{s}_{n'}$ within one step in IT operating mode
$p_{\vec{s}_n \to \vec{s}_{n'}}$	Transition probability to transfer from $\vec{s}_n$ to $\vec{s}_{n'}$ within one step
p_i^n	Probability that the source S_i satisfying $l_i^n \geq l_S^{th}$ to be selected for information transmission at state $\vec{s}_n$
$\mathbf{n}_1$	The $K-$length vector with its kth element satisfying $n_{1,k} \in \{0,1\}$ for $k \in \vartheta_n^{TH} \setminus \{i\}$
$\tau_{1,K}^i$	Set of all qualified $\mathbf{n}_1$
$\vartheta_{n'}^L$	Set of sources whose energy level is L at state $\vec{s}_{n'}$
$\mathbf{A}$	State transition matrix
$\boldsymbol{\pi}$	Stationary distribution vector
$\boldsymbol{\pi}_n$	Stationary probability of state $\vec{s}_n$
P_{EO}	EOP of the network
P_{CO}	COP of the network
$P_{CO,n}$	State COP of the network at state $\vec{s}_n$
R_t	Transmission rate of the network
$p_{T,i}$	Average transmission probability for source S_i
$\bar{T}_i$	ATD of source S_i
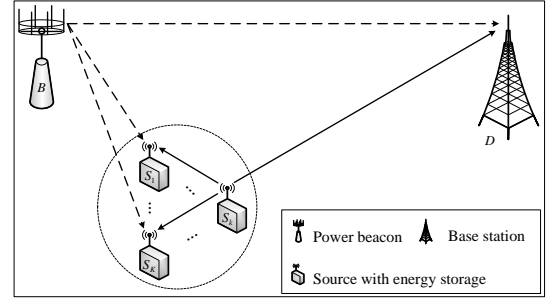
Fig. 1. System model

the network, and the lth energy level is defined as

$$\varepsilon_l = l \cdot \varepsilon_\Delta, \quad l \in \{0, 1, \cdots, L\}, \tag{1}$$

where $\varepsilon_\Delta = \frac{\varepsilon_T}{L}$ is the single unit of energy. For instance, if the new energy arrival from the harvested energy at the kth source node is ε_k, the amount of energy that can be saved in the energy storage after discretization can be expressed as [22, 24]

$$\tilde{\varepsilon}_k = \varepsilon_{l*}, \text{with } l* = \underset{l \in \{0,1,\cdots,L\}}{\arg\max} \{\varepsilon_l : \varepsilon_l \leq \varepsilon_k\}. \tag{2}$$

Recall that there are K storages and each storage has $(1+L)$ levels, thus we have N states in total with $N = (1+L)^K$. The energy level indexes in all the storages form an energy state set $\Theta = \{\vec{s}_1, \cdots, \vec{s}_n, \cdots, \vec{s}_N\}$, where the nth state is given by

$$\vec{s}_n = [l_1^n, \cdots, l_k^n, \cdots, l_K^n], \tag{3}$$

with $n \in \{1, \cdots, N\}$ and $l_k^n \in \{0, 1, \cdots, L\}$ representing the energy level index of kth storage at state $\vec{s}_n$.

B. Network Operating Modes

At any given time, the network is under one specific energy state, and different operating modes are adopted in different states. When the source does not have enough energy to support the IT operation, we define this source as energy outage. When all the sources experience the energy outage at the same time, we define the multi-source network as energy outage. As a result, we assume two operating modes: 1) the network operates in IT mode when there is at least one source that can perform IT operation; and 2) the network operates in non-IT mode when all the sources are in energy outage. Next, we describe the operating mode selection procedure, and the transmission formulation for each operating mode.

1) Operating Mode Selection: We select the operating mode based on the distributed selection method [30, 31]. At the start of each time slot, a pilot signal is broadcasted by D. Using this pilot signal, all the sources that are not in energy outage as well as the PB can individually estimate the channel power gains between themselves and D. For each source that is not in energy outage, its timer with a parameter inversely proportional to its own channel power gain is switched on, namely, the timer of source S_k has the parameter of $C_0 / |h_{S_k D}|^2$, where $h_{S_k D}$ denotes the channel

coefficient between S_k and D, and C_0 is a constant and is properly set to ensure that the shortest duration among all the timers always finishes within the given duration [30, 31]. Once the shortest timer expires, the corresponding source sends a short flag signal to declare its existence, and all the other sources who are waiting for their timer expiring will back off when they hear this flag signal from another source and start to harvest energy. At the same time, D will get ready for receiving useful information upon hearing this flag signal.

For the source that is in energy outage, it will neither estimate its channel nor set a timer. Hence, if the whole network undergoes energy outage, no flag signal would be produced during this flag signal duration. As a result, the operating mode of the network can be easily determined and known by all the nodes within the network. For the notation convenience, the set of indexes of source nodes that are in IT mode at state $\vec{s}_n$ are defined as

$$\vartheta_n^{TH} = \left\{ k : l_k^n \geq l_S^{th} \right\}, \tag{4}$$

where l_S^{th} denotes the transmit energy level threshold, which is expressed as

$$l_S^{th} = \arg\min_{l \in \{1,\cdots,L\}} \left\{ \varepsilon_l : \varepsilon_l \geq \varepsilon_S^{th} \right\}, \tag{5}$$

where ε_S^{th} denotes the transmit energy threshold of sources. Besides, the number of elements in ϑ_n^{TH} is denoted as K_n^{TH}.

2) Non-IT Operating Mode: When the network remains at the Non-IT operating mode, we have $\vartheta_n^{TH} = \Phi_0$, where Φ_0 is the empty set. As described above, no information could be transmitted and all of the sources will harvest energy from the wireless signal transmitted by B. Specifically, the harvested energy at the kth source at state $\vec{s}_n$ is expressed as

$$\varepsilon_k^n = \eta T_0 P_B \left| \mathbf{h}_{BS_k}^T \mathbf{w}_1 \right|^2, \tag{6}$$

where η represents the energy conversion efficiency, and P_B denotes the transmit power of PB. $\mathbf{h}_{BS_k} = \left[h_{B_1 S_k}, \cdots, h_{B_b S_k}, \cdots, h_{B_{N_B} S_k} \right]^T$ represents the channel coefficient vector between B and S_k, $k \in \{1,\cdots,K\}$, $b \in \{1,\cdots,N_B\}$. $\mathbf{w}_1 \in \mathbb{C}^{N_B \times 1}$ is the normalized weight vector applied at B with its bth element satisfying $w_{1,b} = 1/\sqrt{N_B}$. The amount of harvested energy that can be saved in the kth energy storage after discretization, $\tilde{\varepsilon}_k^n$, can be obtained according to (2) by making an appropriate replacement, namely $\varepsilon_k \to \varepsilon_k^n$, $\tilde{\varepsilon}_k \to \tilde{\varepsilon}_k^n$.

3) IT Operating Mode: When the network remains at the IT operating mode, we have $\vartheta_n^{TH} \neq \Phi_0$. As such, a source that has the largest channel power gain is selected for IT operation among all the satisfied sources. Mathematically, the index of the selected source can be given by

$$i^* = \arg\max_{k \in \vartheta_n^{TH}} \left\{ |h_{S_k D}|^2 \right\}. \tag{7}$$

Enjoying the energy harvested from B, the source to destination transmission may also suffer from interference brought by the wireless signals delivered by B. Note that B has also estimated the channel between itself and D with the pilot signal. To exploit the advantages of multiple antennas, the ZF beamforming scheme can be used at B

to fully avoid the interference from B to D. To be specific, a normalized weight vector $\mathbf{w}_2 \in \mathbb{C}^{N_B \times 1}$ satisfying $\mathbf{w}_2 = \mathbf{h}_{BD}^\dagger$ is applied at B so as to keep $\mathbf{h}_{BD}^T \mathbf{w}_2 = 0$, where $\mathbf{h}_{BD} = \left[h_{B_1 D}, \cdots, h_{B_b D}, \cdots, h_{B_{N_B} D} \right]^T$ represents the channel coefficient vector between B and D, and $(\cdot)^\dagger$ denotes the orthogonal operation. Hence, the received SNR at D at state $\vec{s}_n$ when S_{i^*} is selected is given by

$$\gamma_D^{n,i^*} = \frac{P_S}{N_0} |h_{S_{i^*} D}|^2, \tag{8}$$

where N_0 is the power density of the additive white Gaussian noise (AWGN), and P_S represents the transmit power of sources with[2]

$$P_S = l_S \frac{\varepsilon_\Delta}{T_0}, \tag{9}$$

where l_S is the actual transmit energy level satisfying $l_S^{th} \leq l_S \leq L$.

At the same time, all the other sources except S_{i^*} harvest energy from wireless signals, and the harvested energy at the kth source at state $\vec{s}_n$ on condition that S_{i^*} is selected for IT could be expressed as

$$\varepsilon_k^{n,i^*} = \eta T_0 \left(P_S |h_{S_{i^*} S_k}|^2 + P_B \left| \mathbf{h}_{BS_k}^T \mathbf{w}_2 \right|^2 \right), \tag{10}$$

where $k \in \{1,\cdots,K\} \setminus \{i^*\}$, and the amount of harvested energy that can be saved in the kth energy storage after discretization, $\tilde{\varepsilon}_k^{n,i^*}$, can be derived according to (2) by making an appropriate replacement, namely $\varepsilon_k \to \varepsilon_k^{n,i^*}$, $\tilde{\varepsilon}_k \to \tilde{\varepsilon}_k^{n,i^*}$.

III. ENERGY STATE TRANSITIONS

In this section, we present a thorough study on the transitions of the energy states. Let us denote $\vec{s}_n$ and $\vec{s}_{n'}$ as the states at the current and the next time slots, respectively, $n, n' \in \{1,\cdots,N\}$. We then denote the transition probability to transfer from $\vec{s}_n$ to $\vec{s}_{n'}$ within one step as $p_{\vec{s}_n \to \vec{s}_{n'}}$. For the notation convenience, the non-IT set of states Θ_1 and the IT set of states Θ_2 are defined as

$$\Theta_1 = \left\{ \vec{s}_n : \forall n, \text{s.t.} \vartheta_n^{TH} = \Phi_0 \right\}, \tag{11}$$

and

$$\Theta_2 = \left\{ \vec{s}_n : \forall n, \text{s.t.} \vartheta_n^{TH} \neq \Phi_0 \right\}, \tag{12}$$

respectively. Note that Θ_1 represents the set of states that all the sources have to conduct EH operation. In other words, we have $\Theta_1 = \{[0,\cdots,0],\cdots,[(l_S - 1),\cdots,(l_S - 1)]\}$. Besides, Θ_2 is the set of states that at least one source can perform IT operation. It is obvious that Θ_1 is the complement set of Θ_2, so the numbers of states in Θ_1 and Θ_2 are $N_1 = (l_S)^K$ and $N_2 = N - (l_S)^K$, respectively. The energy level increment vector between two states is defined as

$$\Delta \vec{s}_n = \vec{s}_{n'} - \vec{s}_n = [\Delta l_1^n, \cdots, \Delta l_k^n, \cdots, \Delta l_K^n], \tag{13}$$

where $\Delta l_k^n = l_k^{n'} - l_k^n$, and $l_k^{n'}, l_k^n \in \{0, 1, \cdots, L\}$.

---

[2]It is noted that the extra power consumption of the transmitting/receiving circuitry is neglected in this paper [8, 11].
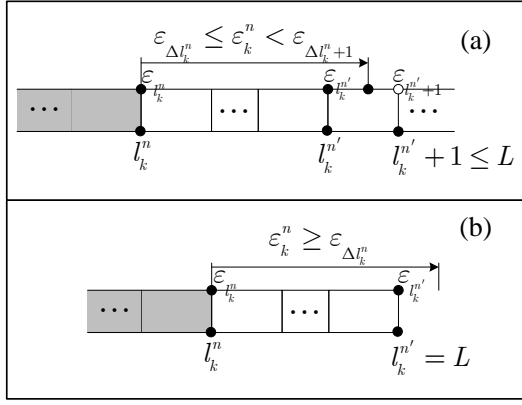
Fig. 2. State transition when (a) $l_k^{n'} \neq L$ and (b) $l_k^{n'} = L$.

Note that when the network operates in the non-IT mode, the energy level in any of the sources will not decline. Hence, it is not possible to transfer from $\vec{s}_n$ to $\vec{s}_{n'}$ within one step if $\vec{s}_{n'} \notin \Theta_1^{n,n'}$, where $\Theta_1^{n,n'}$ is a subset of Θ which satisfies $\Theta_1^{n,n'} = \{\vec{s}_{n'} : \forall k, s.t. \Delta l_k^n \geq 0\}$. It is noted that the construction of $\Theta_1^{n,n'}$ relies on a specific $\vec{s}_n$. Similarly, when the network operates in the IT mode, the energy level in any of the sources except for the selected one S_{i^*} will not decline, and the energy level of S_{i^*} will decline l_S^{th} due to the IT operation. Hence, it is not possible to transfer from $\vec{s}_n$ to $\vec{s}_{n'}$ within one step if $\vec{s}_{n'} \notin \Theta_2^{n,n',i^*}$, where Θ_2^{n,n',i^*} is a subset of Θ which satisfies $\Theta_2^{n,n',i^*} = \{\vec{s}_{n'} : \Delta l_{i^*}^n = -l_S^{th}; \forall k \neq i^*, \Delta l_k^n \geq 0\}$.

A. State Transition When Operating in Non-IT Mode

If the network works in the non-IT mode, namely $\vec{s}_n \in \Theta_1$. Then the probability of the kth source S_k to transfer from l_k^n to $l_k^{n'}$ within one step can be expressed as

$$p_k^{n \to n'} = \Pr\left(\vec{s}_{n'}(k) = l_k^{n'} | \vec{s}_n(k) = l_k^n\right). \quad (14)$$

As mentioned before, $p_k^{n \to n'} = 0$ is always true when $\Delta l_k^n < 0$ in non-IT mode. For the case with $\Delta l_k^n \geq 0$, we will show that $p_k^{n \to n'}$ differs when $l_k^{n'} = L$ and $l_k^{n'} \neq L$, which imply the state after transition for S_k is full and not full, respectively. On one hand, if $l_k^{n'} \neq L$, as shown in Fig. 2 (a), l_k^n can transfer to $l_k^{n'}$ within one step only when the harvested energy, ε_k^n, satisfying $\varepsilon_{\Delta l_k^n} \leq \varepsilon_k^n < \varepsilon_{\Delta l_k^n + 1}$. On the other hand, if $l_k^{n'} = L$, as shown in Fig. 2 (b), it will transfer from l_k^n to $l_k^{n'}$ within one step only when the harvested energy ε_k^n satisfying $\varepsilon_k^n \geq \varepsilon_{\Delta l_k^n}$, which means the harvested energy overflows the remaining storage capacity of this source. Hence, we formulate the transition probability of the kth source as

$$p_k^{n \to n'} = \begin{cases} F_{\varepsilon_k^n}\left(\varepsilon_{\Delta l_k^n + 1}\right) - F_{\varepsilon_k^n}\left(\varepsilon_{\Delta l_k^n}\right), & l_k^{n'} \neq L, \\ 1 - F_{\varepsilon_k^n}\left(\varepsilon_{\Delta l_k^n}\right), & l_k^{n'} = L. \end{cases} \quad (15)$$

When $\vec{s}_n \in \Theta_1$, as each source harvests energy independently, the transition probability of all the sources $p_{\vec{s}_n \to \vec{s}_{n'}}^1$ can be expressed as

$$p_{\vec{s}_n \to \vec{s}_{n'}}^1 = \prod_{k=1}^K p_k^{n \to n'}. \quad (16)$$

To derive $p_{\vec{s}_n \to \vec{s}_{n'}}^1$, we present the following Lemma.

Lemma 1. *The CDF of energy harvested at the kth source with the nth state ε_k^n is derived as*

$$F_{\varepsilon_k^n}(x) = 1 - \exp\left(-\frac{x}{\eta T_0 P_B \bar{\gamma}_{BS_k}}\right). \quad (17)$$

Proof: We first present the CDF as

$$F_{\varepsilon_k^n}(x) = \Pr(\eta T_0 P_B |\mathbf{h}_{BS_k}^T \mathbf{w}_1|^2 \leq x)$$
$$= \Pr\left(\eta T_0 P_B \left|\sum_{b=1}^{N_B} h_{B_b S_k} w_{1,b}\right|^2 \leq x\right)$$
$$= \Pr(\eta T_0 X_1 \leq x) = \Pr\left(X_1 \leq \frac{x}{\eta T_0}\right) \quad (18)$$

where $X_1 = P_B \left|\sum_{b=1}^{N_B} h_{B_b S_k} w_{1,b}\right|^2$. With Rayleigh fading $h_{B_b S_k} \sim \mathcal{CN}(0, \bar{\gamma}_{BS_k})$ and $w_{1,b} = 1/\sqrt{N_B}$ with $b \in \{1, \cdots, N_B\}$, we have $\sum_{b=1}^{N_B} h_{B_b S_k} w_{1,b} = \frac{1}{\sqrt{N_B}} \sum_{b=1}^{N_B} h_{B_b S_k}$. It is noted that the sum of finite Gaussian random variables is still a Gaussian random variable [32], hence $\sum_{b=1}^{N_B} h_{B_b S_k} \sim \mathcal{CN}(0, N_B \bar{\gamma}_{BS_k})$, which results in $\frac{1}{\sqrt{N_B}} \sum_{b=1}^{N_B} h_{B_b S_k} \sim \mathcal{CN}(0, \bar{\gamma}_{BS_k})$. Therefore, X_1 is an exponentially distributed random variable with the mean of $P_B \bar{\gamma}_{BS_k}$ with

$$f_{X_1}(y) = \frac{1}{P_B \bar{\gamma}_{BS_k}} \exp\left(-\frac{y}{P_B \bar{\gamma}_{BS_k}}\right). \quad (19)$$

Substituting (19) into (18), we prove (17). ∎

By substituting (15) and (17) into (16), the transition probability of all sources from $\vec{s}_n$ to $\vec{s}_{n'}$ in non-IT mode for $\vec{s}_{n'} \in \Theta_1^{n,n'}$ can be derived as

$$p_{\vec{s}_n \to \vec{s}_{n'}}^1 = e^{-\frac{\varepsilon_{\Delta l_k^n}}{\eta T_0 P_B \bar{\gamma}_{BS_k}}} \prod_{\substack{k=1 \\ k \notin \vartheta_{n'}^L}}^K \left(1 - e^{-\frac{\varepsilon_1}{\eta T_0 P_B \bar{\gamma}_{BS_k}}}\right). \quad (20)$$

B. State Transition When Operating in IT Mode

If the network works in IT-mode, namely $\vec{s}_n \in \Theta_2$. We further assume the condition that $i^* = i$, namely the transfer from $\vec{s}_n$ to $\vec{s}_{n'}$ results from the IT selection of S_i. Correspondingly, we have $\Theta_2^{n,n',i^*} = \Theta_2^{n,n',i} = \{\vec{s}_{n'} : \Delta l_i^n = -l_S^{th}; \forall k \neq i, \Delta l_k^n \geq 0\}$ on this condition. Then the transition probability of the kth source to transfer from $\vec{s}_n$ to $\vec{s}_{n'}$ within one step is derived as

$$p_k^{n \to n',i} = \begin{cases} F_{\varepsilon_k^{n,i}}\left(\varepsilon_{\Delta l_k^n + 1}\right) - F_{\varepsilon_k^n}\left(\varepsilon_{\Delta l_k^n}\right), & l_k^{n'} \neq L, \\ 1 - F_{\varepsilon_k^{n,i}}\left(\varepsilon_{\Delta l_k^n}\right), & l_k^{n'} = L. \end{cases} \quad (21)$$

As such, the transition probability of all sources from $\vec{s}_n$ to $\vec{s}_{n'}$ in the IT mode can be written as

$$p_{\vec{s}_n \to \vec{s}_{n'}}^2 = p_i^n \prod_{\substack{k=1 \\ k \neq i}}^K p_k^{n \to n',i}. \quad (22)$$

To derive the source selection probability p_i^n, we present the following Lemma.

Lemma 2. *For the IT mode $\vec{s}_n \in \Theta_2$, the probability that the source S_i satisfying $l_i^n \geq l_S^{th}$ to be selected for information transmission $p_i^n = \Pr\left(S_{i^*} = S_i\right)$ is derived as*

$$p_i^n = \sum_{\mathbf{n}_1 \in \tau_{1,K}^i} \frac{(-1)^{\sum_{k=1}^K n_{1,k}}}{\bar{\gamma}_{S_i D} \sum_{k=1}^K \frac{n_{1,k}}{\bar{\gamma}_{S_k D}} + 1}, \qquad (23)$$

where $\mathbf{n}_1$ is the $K-$length vector with its kth element satisfying $n_{1,k} \in \{0,1\}$ for $k \in \vartheta_n^{TH} \backslash \{i\}$, $\tau_{1,K}^i$ is the set of all qualified $\mathbf{n}_1$, and $n_{2,k} = 0$ for $k \notin \vartheta_n^{TH}$ and $k = i$.

Proof: When $l_i^n \geq l_S^{th}$, we denote $Z_i = |h_{S_i D}|^2$, and $Z'_i = \max_{k \in \vartheta_n^{TH} \backslash \{i\}} \{Z_k\}_{k=1}^K$ with $i \in \vartheta_n^{TH}$, then p_i^n is given as $p_i^n = \Pr\left(Z_i > Z'_i\right)$, which can be calculated as

$$p_i^n = \int_0^\infty F_{Z'_i}(z) f_{Z_i}(z) \, dz. \qquad (24)$$

We first derive

$$F_{Z'_i}(z) = \prod_{\substack{k \in \vartheta_n^{TH} \backslash \{i\}}}^K \left(1 - e^{-\frac{z}{\bar{\gamma}_{S_k D}}}\right). \qquad (25)$$

Referring to [33], $F_{Z'_i}(z)$ can be rewritten as

$$F_{Z'_i}(z) = \sum_{\mathbf{n}_1 \in \tau_{1,K}^i} \prod_{k=1}^K (-1)^{n_{1,k}} e^{-\frac{n_{1,k}}{\bar{\gamma}_{S_k D}} z}$$

$$= \sum_{\mathbf{n}_1 \in \tau_{1,K}^i} (-1)^{\sum_{k=1}^K n_{1,k}} e^{-z \sum_{k=1}^K \frac{n_{1,k}}{\bar{\gamma}_{S_k D}}}. \qquad (26)$$

In addition, we know that

$$f_{Z_i}(z) = \frac{1}{\bar{\gamma}_{S_i D}} e^{-\frac{z}{\bar{\gamma}_{S_i D}}}. \qquad (27)$$

Substituting (26) and (27) into (24), and after some simple manipulations, (23) can be readily derived. ∎

To derive the transition probability of the kth source from $\vec{s}_n$ to $\vec{s}_{n'}$ in the IT mode, we present the following lemma.

Lemma 3. *The CDF of the energy harvested at the kth source with the nth state ε_k^{n,i^*} is derived as*

$$F_{\varepsilon_k^{n,i^*}}(x) = 1 - e^{-\frac{x}{\eta T_0 P_B \bar{\gamma}_{BS_k}}} - \frac{P_S \bar{\gamma}_{S_{i^*} S_k}}{P_B \bar{\gamma}_{BS_k} - P_S \bar{\gamma}_{S_{i^*} S_k}}$$

$$\times \left(e^{\mu_1 \frac{x}{\eta T_0}} - 1\right) e^{-\frac{x}{\eta T_0 P_S \bar{\gamma}_{S_{i^*} S_k}}}, \qquad (28)$$

where $\mu_1 = \frac{P_B \bar{\gamma}_{BS_k} - P_S \bar{\gamma}_{S_{i^*} S_k}}{P_S \bar{\gamma}_{S_{i^*} S_k} P_B \bar{\gamma}_{BS_k}}$.

Proof: We first present the CDF of ε_k^{n,i^*} as

$$F_{\varepsilon_k^{n,i^*}}(x) = \Pr\left(\eta T_0 \left(P_S |h_{S_{i^*} S_k}|^2 + P_B |\mathbf{h}_{BS_k}^T \mathbf{w}_2|^2\right) \leq x\right)$$

$$= \Pr(X_2 + X_3 \leq \frac{x}{\eta T_0})$$

$$= \int_0^{\frac{x}{\eta T_0}} F_{X_2}\left(\frac{x}{\eta T_0} - y\right) f_{X_3}(y) \, dy, \qquad (29)$$

where $X_2 = P_S |h_{S_{i^*} S_k}|^2$ and $X_3 = P_B \left|\sum_{b=1}^{N_B} h_{B_b S_k} w_{2,b}\right|^2$. With $\mathbf{w}_2 = \mathbf{h}_{BD}^\dagger$, the construction of $\mathbf{w}_2$ is independent with $\mathbf{h}_{BS_k}$, so we have $\sum_{b=1}^{N_B} h_{B_b S_k} w_{2,b} \sim$

$\mathcal{CN}\left(0, \bar{\gamma}_{BS_k} \sum_{b=1}^{N_B} |w_{2,b}|^2\right)$ with $\sum_{b=1}^{N_B} |w_{2,b}|^2 = 1$ [32]. As a result, the PDF of X_3 is derived as

$$f_{X_3}(y) = \frac{1}{P_B \bar{\gamma}_{BS_k}} \exp\left(-\frac{y}{P_B \bar{\gamma}_{BS_k}}\right). \qquad (30)$$

Besides, we know that $X_2 \sim \exp\left(P_S \bar{\gamma}_{S_{i^*} S_k}\right)$, and its CDF is written as

$$F_{X_2}(x) = 1 - \exp\left(-\frac{x}{P_S \bar{\gamma}_{S_{i^*} S_k}}\right). \qquad (31)$$

Substituting (30) and (31) into (29), we prove (28) in Lemma 3. ∎

By utilizing the results in Lemmas 2 and 3, the transition probability from $\vec{s}_n$ to $\vec{s}_{n'}$ in IT mode when $\vec{s}_{n'} \in \Theta_2^{n,n',i}$ can be derived as

$$p_{\vec{s}_n \to \vec{s}_{n'}}^2 = \sum_{\mathbf{n}_1 \in \tau_{1,K}^i} \frac{(-1)^{\sum_{k=1}^K n_{1,k}}}{\bar{\gamma}_{S_i D} \sum_{k=1}^K \frac{n_{1,k}}{\bar{\gamma}_{S_k D}} + 1}$$

$$\times \prod_{\substack{k=1 \\ k \neq i, \\ k \in \vartheta_{n'}^L}}^K \Lambda_1(i,k)$$

$$\times \prod_{\substack{k=1 \\ k \neq i, \\ k \notin \vartheta_{n'}^L}}^K \Lambda_2(i,k), \qquad (32)$$

with

$$\Lambda_1(i,k) = e^{-\frac{\varepsilon_{\Delta l_k^n}}{\eta T_0 P_B \bar{\gamma}_{BS_k}}} + \frac{P_S \bar{\gamma}_{S_i S_k}}{P_B \bar{\gamma}_{BS_k} - P_S \bar{\gamma}_{S_i S_k}}$$

$$\times e^{-\frac{\varepsilon_{\Delta l_k^n}}{\eta T_0 P_S \bar{\gamma}_{S_i S_k}}} \left(e^{\mu_1 \frac{\varepsilon_{\Delta l_k^n}}{\eta T_0}} - 1\right), \qquad (33)$$

$$\Lambda_2(i,k) = \Lambda_1(i,k) - \frac{P_S \bar{\gamma}_{S_i S_k} e^{-\frac{\varepsilon_{\Delta l_k^n + 1}}{\eta T_0 P_S \bar{\gamma}_{S_i S_k}}}}{P_B \bar{\gamma}_{BS_k} - P_S \bar{\gamma}_{S_i S_k}}$$

$$\times \left(e^{\mu_1 \frac{\varepsilon_{\Delta l_k^n + 1}}{\eta T_0}} - 1\right) - e^{-\frac{\varepsilon_{\Delta l_k^n + 1}}{\eta T_0 P_B \bar{\gamma}_{BS_k}}}, \qquad (34)$$

where $\vartheta_{n'}^L = \left\{k : l_k^{n'} = L\right\}$ represents the set of sources whose energy level is L at state $\vec{s}_{n'}$.

To conclude, the transition probability from $\vec{s}_n$ to $\vec{s}_{n'}$ within one step is summarized as

$$p_{\vec{s}_n \to \vec{s}_{n'}} = \begin{cases} p_{\vec{s}_n \to \vec{s}_{n'}}^1, & \vec{s}_n \in \Theta_1, \vec{s}_{n'} \in \Theta_1^{n,n'}, \\ p_{\vec{s}_n \to \vec{s}_{n'}}^2, & \vec{s}_n \in \Theta_2, \vec{s}_{n'} \in \Theta_2^{n,n',i}, \\ 0, & others. \end{cases} \qquad (35)$$

Let us denote $\mathbf{A} \in \mathbb{R}^{N \times N}$ as the state transition matrix of the proposed network, where the (n, n')th element $a_{n,n'}$ represents the probability to transfer from $\vec{s}_n$ to $\vec{s}_{n'}$, and is given by

$$a_{n,n'} = p_{\vec{s}_n \to \vec{s}_{n'}}. \qquad (36)$$

We then formulate the stationary distribution vector $\boldsymbol{\pi} \in \mathbb{R}^{N \times 1}$ for the energy states, where its nth element, $\boldsymbol{\pi}_n$, stands for the stationary probability of state $\vec{s}_n$ for the network. It can be easily verified that each state can be transfered from
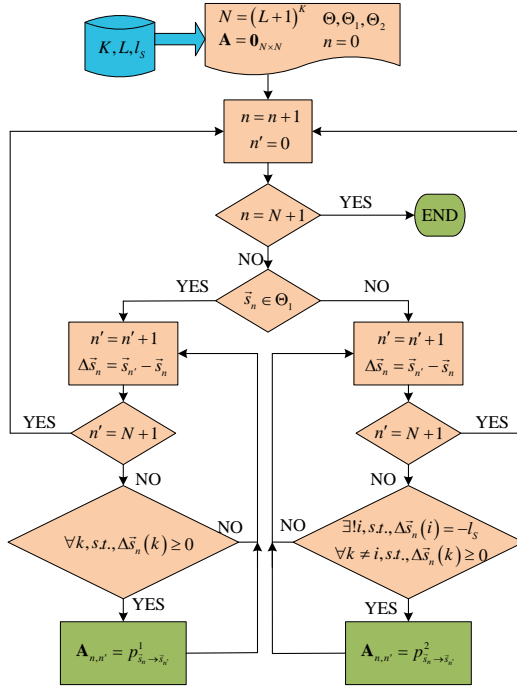
Fig. 3. Flow diagram for the generation of the state transition matrix **A**.
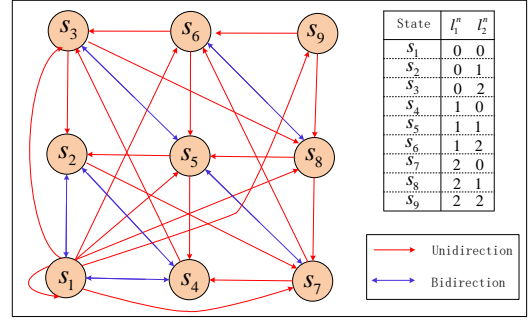

Fig. 4. State diagram of the Markov chain representing the states of the storages and the transitions between them for a case with $K = 2$ and $L = 2$.

TABLE II
ILLUSTRATION OF EXAMPLE WHEN $K = 2$, $L = 2$.

State s_n	$[l_1^n, l_2^n]$	π_n	$[p_1^n, P_2^n]$	State COP
s_1	[0,0]	0.0220	[0,0]	0
s_2	[0,1]	0.0434	[0,1]	0.0545
s_3	[0,2]	0.1587	[0,1]	0.0545
s_4	[1,0]	0.0640	[1,0]	0.0553
s_5	[1,1]	0.1022	[0.4963,0.5037]	0.0030
s_6	[1,2]	0.1811	[0.4963,0.5037]	0.0030
s_7	[2,0]	0.1998	[1,0]	0.0553
s_8	[2,1]	0.2210	[0.4963,0.5037]	0.0030
s_9	[2,2]	0.0078	[0.4963,0.5037]	0.0030
		EOP	$[p_{T,1}, p_{T,2}]$	Overall COP
Derived results		0.0220	[0.5179,0.4601] $[\bar{T}_1, \bar{T}_2]$ [1.9309,2.1734]	0.0271

others, thus **A** is irreducible. Besides, for any Markov chain, the transition from state s_n to $s_{n'}$ for all possible states s_n sums up to 1, thus **A** is row stochastic [34]. As a consequence, a unique stationary distribution must exist that satisfies [22, 34]

$$\pi = \mathbf{A}^T \pi. \qquad (37)$$

According to [34, Eq. (12)], the solve of (37) could be derived as

$$\pi = \left(\mathbf{A}^T - \mathbf{E} + \mathbf{Q}\right)^{-1} \mathbf{b}, \qquad (38)$$

where $\mathbf{b} = (1, 1, \cdots 1)^T$, $\mathbf{E}$ is the identity matrix, and $\mathbf{Q}$ is an all-ones matrix.

For a better comprehension, Fig. 3 depicts the block diagram for the construction of the state transition matrix **A** based on the system parameters K, L and l_S. Fig. 4 illustrates the transitions of the states for a simple example with $K = 2$ and $L = 2$. The corresponding state transition matrix **A** could be derived as (39). By applying the described approach, the stationary state probabilities of all the states, as well as the EOP, COP and ATD for S_1 and S_2 are obtained as shown in Table II. The related parameters are set as $P_B = 30$ dBm, $\varepsilon_T = 20$ mJ, $\varepsilon_S^{th} = 10$ mJ, $l_S = l_S^{th}$, $\eta = 0.8$, $R_t = 3$ bits/s/Hz, $x_B = -3$ m, $x_D = 200$ m, $r_S = 1$ m, $N_B = 5$, $N_0 = -80$ dBm, and $\alpha = 3$. The coordinates of B and D as well as S_1 and S_2 are $B = (-3, 0)$, $D = (200, 0)$, $S_1 = (-1, 0)$ and $S_2 = (0, 1)$, respectively. The unit of distance is the meter.

IV. OUTAGE AND DELAY

In this section, we characterize the performance in terms of outage and delay. To reveal key insights of the proposed network, we derive exact expressions for the EOP, COP, and ATD of proposed networks.

A. Energy Outage Probability

In the proposed network, the EOP is defined as the network energy outage in the non-IT mode when all the sources experience energy outage. The EOP is derived as in the following theorem.

Theorem 1. *The EOP for the multi-source WPT network is derived as*

$$P_{EO} = \sum_{\vec{s}_n \in \Theta_1} \pi_n, \qquad (40)$$

where π_n has been derived as in (38).

Proof: According to the definition of the network energy outage given in II-B, the EOP of the proposed network is readily derived. ∎

Corollary 1. *The EOP for the multi-source WPT network when the transmit power of the PB goes to infinity ($P_B \to \infty$) is given by*

$$P_{EO} = \begin{cases} \sum_{\vec{s}_n \in \Theta_1} \pi_n, & K = 1, \\ 0, & K \geq 2, \end{cases} \qquad (41)$$

where π_n has been derived as in (38).

$$\mathbf{A} = \begin{pmatrix} 0.0356 & 0.0237 & 0.0471 & 0.0318 & 0.0212 & 0.0421 & 0.2674 & 0.1779 & 0.3533 \\ 0.0851 & 0 & 0 & 0.0972 & 0 & 0 & 0.8177 & 0 & 0 \\ 0 & 0.0851 & 0 & 0 & 0.0972 & 0 & 0 & 0.8177 & 0 \\ 0.2737 & 0.2427 & 0.4836 & 0 & 0 & 0 & 0 & 0 & 0 \\ 0 & 0.1358 & 0.3604 & 0.0429 & 0 & 0 & 0.4609 & 0 & 0 \\ 0 & 0 & 0.4963 & 0 & 0.0429 & 0 & 0 & 0.4609 & 0 \\ 0 & 0 & 0 & 0.2737 & 0.2427 & 0.4836 & 0 & 0 & 0 \\ 0 & 0 & 0 & 0 & 0.1358 & 0.3604 & 0.5037 & 0 & 0 \\ 0 & 0 & 0 & 0 & 0 & 0.4963 & 0 & 0.5037 & 0 \end{pmatrix}. \tag{39}$$

Proof: We first denote $\mathbf{A} = \begin{pmatrix} \mathbf{A}_{1,1} & \mathbf{A}_{1,2} \\ \mathbf{A}_{2,1} & \mathbf{A}_{2,2} \end{pmatrix}$, where $\mathbf{A}_{i,j}$ represents the transition matrix from Θ_i to Θ_j, $i, j \in \{1, 2\}$. We also denote the stationary distributions of states in Θ_1 and Θ_2 as $\boldsymbol{\pi}_1^\Theta \in \mathbb{R}^{N_1 \times 1}$ and $\boldsymbol{\pi}_2^\Theta \in \mathbb{R}^{N_2 \times 1}$, respectively.

When $P_B \to \infty$, we have $\varepsilon_k^n \to \infty$, $\varepsilon_k^{n,i^*} \to \infty$. Therefore, if $\vec{s}_n \in \Theta_1$, it will always transfer to the all-full state $[L, \cdots, L]$, because the harvested energy at each source will always exceed the energy capacity. Similarly, if $\vec{s}_n \in \Theta_2$, it will always transfer to an almost-all-full state $[L, \cdots, l_{i^*}, \cdots, L]$, where $0 \le l_{i^*} \le L - l_S$ and $i^* \in \{1, \cdots, K\}$ is the index of the selected IT source. Note that both $[L, \cdots, L]$ and $[L, \cdots, l_{i^*}, \cdots, L]$ are an element of Θ_2. As a result, for $K \ge 2$, regardless of any current state the network remains, it will never transfer to Θ_1, which results to $\mathbf{A}_{1,1} = \mathbf{0}_{N_1 \times N_1}$ and $\mathbf{A}_{2,1} = \mathbf{0}_{N_2 \times N_1}$. Substituting the derived results into (37), we derive the matrix-form equation as

$$\begin{pmatrix} \mathbf{0}_{N_1 \times N_1} & \mathbf{A}_{1,2} \\ \mathbf{0}_{N_2 \times N_1} & \mathbf{A}_{2,2} \end{pmatrix}^T \begin{pmatrix} \boldsymbol{\pi}_1^\Theta \\ \boldsymbol{\pi}_2^\Theta \end{pmatrix} = \begin{pmatrix} \boldsymbol{\pi}_1^\Theta \\ \boldsymbol{\pi}_2^\Theta \end{pmatrix}, \tag{42}$$

which yields to $\boldsymbol{\pi}_1^\Theta = \mathbf{0}$. Referring to (40), we derive the EOP of the network as

$$P_{EO} = \sum_{\vec{s}_n \in \Theta_1} \boldsymbol{\pi}_n = \sum_{k=1}^{N_1} \boldsymbol{\pi}_{1,k}^\Theta = 0, \tag{43}$$

where $\boldsymbol{\pi}_{1,k}^\Theta$ denotes the kth element of $\boldsymbol{\pi}_1^\Theta$.

Whereas, for $K = 1$, due to the half-duplex nature, the single source can not harvest energy when it transmits information. Hence, if the network remains in Θ_2, the source will always consumed energy until an energy outage event occurs. As such, the EOP when $K = 1$ is derived using (40). ∎

B. Connection Outage Probability

The COP quantifies the probability that the information can not be correctly decoded at the legitimate receiver when the IT operation actually takes place. According to the total probability theorem, and considering the fact that no data is transmitted when energy outage occurs.

Theorem 2. *The overall COP for the multi-source WPT network is derived as*

$$P_{CO} = \sum_{\vec{s}_n \in \Theta_2} \boldsymbol{\pi}_n \prod_{k \in \vartheta_n^{TH}}^K \left(1 - \exp\left(-\frac{\sigma_D^2 \gamma_{th}^t}{\bar{\gamma}_{S_k D} P_S} \right) \right), \tag{44}$$

where $\boldsymbol{\pi}_n$ has been derived as in (38).

Proof: According to the total probability theorem, the overall COP of the multi-source WPT network can be calculated as

$$P_{CO} = \sum_{\vec{s}_n \in \Theta} \boldsymbol{\pi}_n P_{CO,n} \overset{(a)}{=} \sum_{\vec{s}_n \in \Theta_2} \boldsymbol{\pi}_n P_{CO,n}. \tag{45}$$

where the result after $\overset{(a)}{=}$ is derived according to the fact that no information would be transmitted when energy outage occurs, and $P_{CO,n}$ represents the state COP when the network remains at state $\vec{s}_n$, which is derived as

$$P_{CO,n} = \sum_{i \in \vartheta_n^{TH}} \Pr(i^* = i) \Pr\left(\gamma_D^{n,i^*} < \gamma_{th}^t \right).$$
$$= \sum_{i \in \vartheta_n^{TH}} p_i^n F_{\gamma_D^{n,i^*}} \left(\gamma_{th}^t \right) \tag{46}$$

where $\gamma_{th}^t = 2^{R_t} - 1$, R_t (bits/s/Hz) denotes the transmission rate of the network.

According to the selection policy described in (7), we can present the CDF of γ_D^{n,i^*} as

$$F_{\gamma_D^{n,i^*}}(x) = F_{Y_{SD}} \left(\sigma_D^2 x \right), \tag{47}$$

where $Y_{SD} = P_S \max_{k \in \vartheta_n^{TH}} \left\{ |h_{S_k D}|^2 \right\}$. After some manipulations, the CDF of Y_{SD} is derived as

$$F_{Y_{SD}}(y) = \prod_{k \in \vartheta_n^{TH}}^K \left(1 - \exp\left(-\frac{y}{\bar{\gamma}_{S_k D} P_S} \right) \right). \tag{48}$$

It is easy to find from (47) and (48) that the CDF of γ_D^{n,i^*} has no relationship with the selection probabilities of every source S_i, $i \in \vartheta_n^{TH}$. Besides, according to the total probability theorem, we derive $\sum_{i \in \vartheta_n^{TH}} p_i^n = 1$. Hence, $P_{CO,n}$ can be calculated as

$$P_{CO,n} = F_{\gamma_D^{n,i^*}} \left(\gamma_{th}^t \right)$$
$$= \prod_{k \in \vartheta_n^{TH}}^K \left(1 - \exp\left(-\frac{\sigma_D^2 \gamma_{th}^t}{\bar{\gamma}_{S_k D} P_S} \right) \right). \tag{49}$$

By substituting $\boldsymbol{\pi}_n$ in (38) and $P_{CO,n}$ in (49) into (45), the COP of the proposed network is derived. ∎

C. Average Transmission Delay

In the IT mode, there would be at most one source to send messages at each time slot, a transmission delay is caused at each source. In practical, we may concern that how many time slots on average a specific source need to wait for to be selected for IT operation, which can be quantified by the average transmission delay (ATD).

Before delving into the investigation, we will clarify the fundamental conception of ATD by giving out a simple example. Let us start by looking into the network of K energy-sufficient sources, where all the sources can be selected for IT operation equally. It is readily known that at each time slot, each source has the transmission probability of $1/K$. In other words, for each source, a time slot is allocated once on average within K slots. As a consequence, the ATD would be $\bar{T} = KT_0$ for every source in this network [3]. However, in our proposed energy storage networks, whether a specific source can be selected for IT operation differs for different storage states. In other words, the transmission probability of a certain source is not fixed, and all the sources do not have the equal transmission probability as well.

In order to solve this problem, we denote $p_{T,i}^n$ as the transmission probability for source S_i at state s_n. According to the previous description, $p_{T,i}^n$ can be derived as

$$p_{T,i}^n = \begin{cases} 0, & l_i^n < l_S, \\ p_i^n, & l_i^n \geq l_S. \end{cases} \tag{50}$$

Theorem 3. *The average transmission probability for source S_i and its ATD are derived as*

$$p_{T,i} = \sum_{\vec{s}_n \in \Theta} \boldsymbol{\pi}_n p_{T,i}^n = \sum_{\vec{s}_n \in \Theta_2} \boldsymbol{\pi}_n p_{T,i}^n, \tag{51}$$

and

$$\bar{T}_i = \frac{T_0}{p_{T,i}} = \frac{T_0}{\sum_{\vec{s}_n \in \Theta_2} \boldsymbol{\pi}_n p_{T,i}^n}, \tag{52}$$

respectively, where $\boldsymbol{\pi}_n$ has been derived as in (38).

Proof: The proof is omitted. ∎

V. NUMERICAL RESULTS

In this section, we present the numerical results to illustrate the impacts of various system parameters on the performance of the proposed network. As shown in the below figures, the theoretical results are in exact agreement with the numerical simulations, which show the correctness of the analysis. Without any loss of generality, all the nodes are set in a two-dimensional plane in all simulations, and the coordinates of B and D are set as $B = (x_B, 0)$ and $D = (x_D, 0)$, and the coordinates of the source nodes are assumed to be $S_1 = (-r_S, 0)$, $S_2 = (0, r_S)$, $S_3 = (r_S, 0)$, $S_4 = (0, -r_S)$, $S_5 = (\frac{\sqrt{2}}{2} r_S, \frac{\sqrt{2}}{2} r_S)$ and $S_6 = (-\frac{\sqrt{2}}{2} r_S, -\frac{\sqrt{2}}{2} r_S)$, respectively. With K sources, we take sources from S_1 to S_K in order automatically, and we set $\alpha = 3$, $R_t = 3$ bits/s/Hz, $N_B = 5$, $N_0 = -80$ dBm, and $\varepsilon_S^{th} = 10$ mJ.

---

[3]For the extreme case of $K = 1$, we can find that the source can always transmit successively. We say that the ATD of this network is $\bar{T} = T_0$, even though no time slot is needed to wait for IT operation.
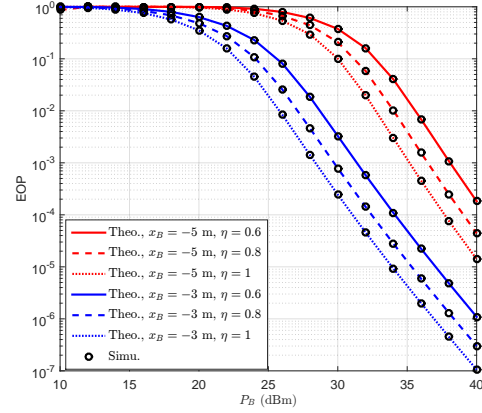

Fig. 5. EOP of the multi-source WPT network versus the transmit power of power beacon P_B with different x_B and η. $K = 2$, $L = 10$, $l_S = l_S^{th}$, $\varepsilon_T = 40$ mJ, $x_D = 200$ m, and $r_S = 1$ m.

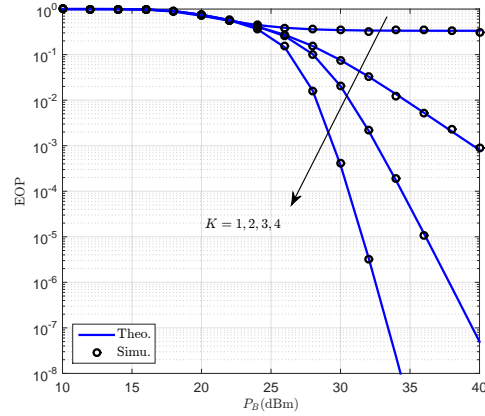
Fig. 6. EOP of the multi-source WPT network versus the transmit power of power beacon P_B with different K. $l_S = l_S^{th}$, $\eta = 0.8$, $\varepsilon_T = 40$ mJ, $L = 2$, $x_B = -3$ m, $x_D = 200$ m, and $r_S = 1$ m.

Fig. 5 plots the EOP of the multi-source WPT network versus the transmit power of the power beacon P_B with different x_B and η. As can be seen from this figure, the EOP declines rapidly when P_B increases. Besides, it shows that the EOP will grow severely when x_B increases. Moreover, the EOP also raises when η becomes smaller. This can be well understood because a greater x_B implies a farther distance of energy transmission, which results in the decline of accessible energy that can be harvested by sources due to a much severer path poss. Likewise, a smaller η means a lower energy efficiency, which indicates that less energy can be converted by sources and saved in their storages.

Fig. 6 plots the EOP of the multi-source WPT network versus the transmit power of the power beacon P_B with different K. It is depicted that, the EOP performance is rather poor when $K = 1$, which however can be greatly improved when multiple sources are deployed, especially when a larger P_B can be provided. This finding is of significant importance because it indicates the effectiveness to greatly decrease the EOP of network by increasing the number of the sources.
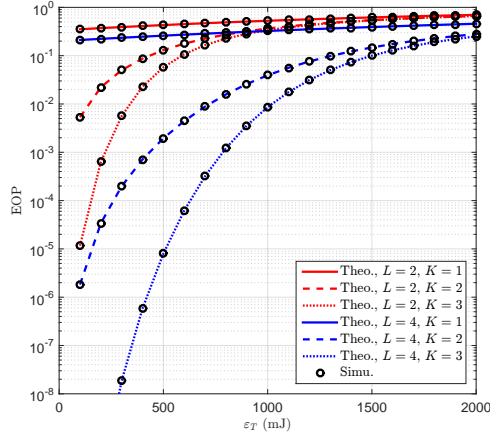
Fig. 7. EOP of the multi-source WPT network versus the energy capacity ε_T with different K and L. $P_B = 30$ dBm, $l_S = l_S^{th}$, $\eta = 0.8$, $x_B = -3$ m, $x_D = 200$ m, and $r_S = 1$ m.
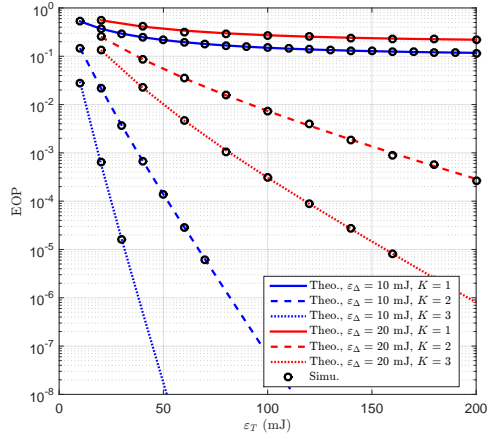

Fig. 9. COP of the multi-source WPT network versus the energy capacity ε_T with different P_B. $K = 2$, $\varepsilon_\Delta = 20$ mJ, $l_S = l_S^{th}$, $\eta = 0.8$, $x_B = -3$ m, $x_D = 200$ m, and $r_S = 1$ m.

Fig. 8. EOP of the multi-source WPT network versus the energy capacity ε_T with different K and ε_Δ. $P_B = 30$ dBm, $l_S = l_S^{th}$, $\eta = 0.8$, $x_B = -3$ m, $x_D = 200$ m, and $r_S = 1$ m.

Fig. 10. COP of the multi-source WPT network versus the energy capacity ε_T with different P_B. $K = 3$, $\varepsilon_\Delta = 20$ mJ, $l_S = l_S^{th}$, $\eta = 0.8$, $x_B = -3$ m, $x_D = 200$ m, and $r_S = 1$ m.

Figs. 7-8 examine the EOP of the multi-source WPT network versus the energy capacity ε_T. We note that in Fig. 7, the discretization level of the network L is fixed so that the single unit of energy ε_Δ grows proportionally with the growth of ε_T. However, in Fig. 8, L and ε_T are proportionally increased while keeping ε_Δ unchanged. From Fig. 7, we find that for a specific ε_T, the EOP reduces when a larger L is applied. By contrast, for a given L, the EOP grows rapidly with the increase of ε_T. Specifically, when ε_T is large enough, the EOP approaches close to 1, even when multiple sources are applied. On the contrary, it is demonstrated in Fig. 8 that, the EOP declines significantly with the increase of ε_T, which differs from the behavior shown in Fig. 7. We note that the harvested energy at each time slot is limited. Therefore, less energy could be harvested for the network when the single unit of energy ε_Δ grows, as a larger ε_Δ is more difficult to be satisfied.

Figs. 9-10 compare the COP of the multi-source WPT network versus the energy capacity ε_T with different P_B. As
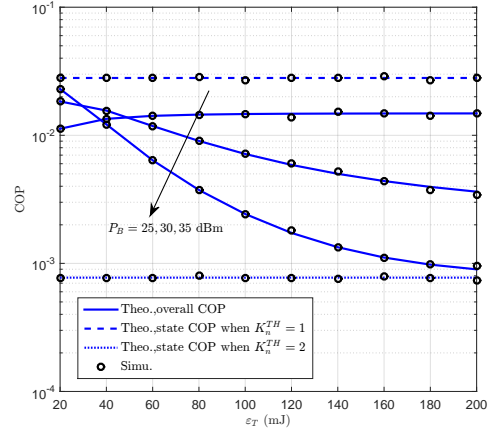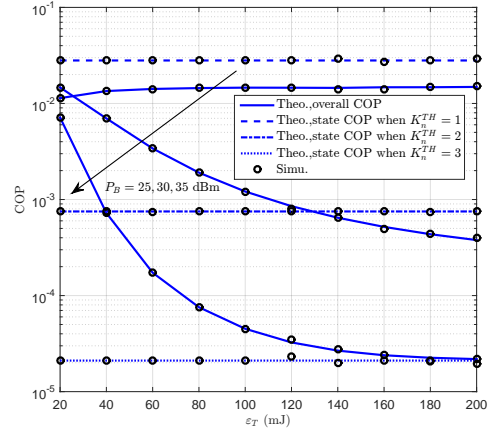
depicted in these figures, the COPs under different states vary greatly, and the overall COP firstly approaches to the worst state performance and then goes down to get close to the best state performance if an appropriate P_B could be provided. Besides, this trend could be accelerated by increasing P_B. All these observations indicate that a greater energy capacity and P_B are both benefit to decrease the overall COP of the network.

Fig. 11 plots the COP of the multi-source WPT network versus the transmit power of the power beacon P_B with different K and x_D. As can be predicted, the COP of the network grows rapidly when x_D increases, which again is resulted from the path loss effect of the wireless channel. In addition, we observe that the COP performance could also be significantly enhanced by adding the number of the sources. It is noted that for a specific line with fixed K and x_D, the COP goes up with the increase of P_B at first and then turns down quickly at about 20 to 25 dBm, which reaches a floor
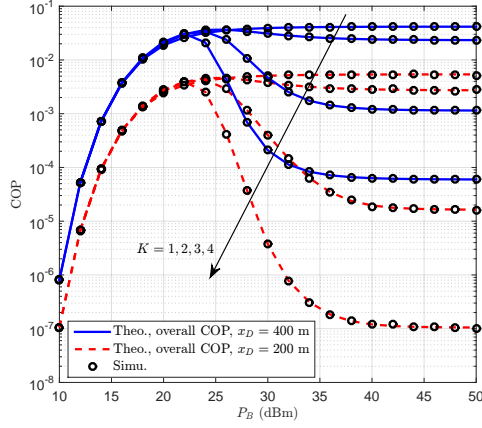
Fig. 11. COP of the multi-source WPT network versus the transmit power of power beacon P_B with different K and x_D. $L = 2$, $\varepsilon_T = 20$ mJ, $l_S = l_S^{th}$, $\eta = 0.8$, $x_B = -3$ m, and $r_S = 1$ m.

Fig. 13. ATD of the multi-source WPT network versus the transmit power of power beacon P_B with different P_S. $K = 2$, $L = 5$, $\varepsilon_T = 50$ mJ, $\eta = 0.8$, $r_S = 0.2$ m, $x_B = -3$ m and $x_D = 200$ m.
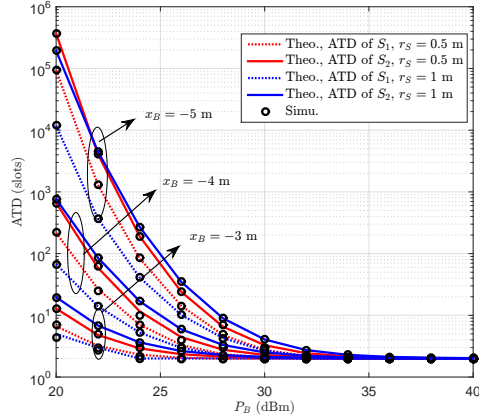

Fig. 12. ATD of the multi-source WPT network versus the transmit power of power beacon P_B with different r_S and x_B. $K = 2$, $L = 2$, $\varepsilon_T = 20$ mJ, $l_S = l_S^{th}$, $\eta = 0.8$, and $x_D = 200$ m.

Fig. 14. ATD of S_1 versus the transmit power of power beacon P_B with different K. $L = 2$, $\varepsilon_T = 20$ mJ, $l_S = l_S^{th}$, $\eta = 0.8$, $r_S = 0.2$ m, $x_B = -4$ m and $x_D = 200$ m.

eventually. We highlight that, as has clarified previously, it is rather difficult for the sources to collect sufficient energy from the wireless signals if P_B remains at a very low level. Hence, the EOP of network would be rather large in this case, so IT operation can only occur with a very little probability. Recalling that the overall COP is the weighted average of all the states, hence, it would be rather low because the network will stay in energy outage state with a very high probability. It should be pointed out that the low level of COP under this condition does not mean a good performance. Instead, it indicates a very poor performance because it will result in a huge transmission delay to the sources.

Figs. 12-13 present the ATD of the multi-source WPT network versus the transmit power of the power beacon P_B with different r_S, x_B and P_S. It is easy to find from these two figures that the ATD performance is not symmetric to all the sources, and this asymmetry would be enlarged when r_S increases. This is comprehensible because in the proposed network, each source undergoes independent but
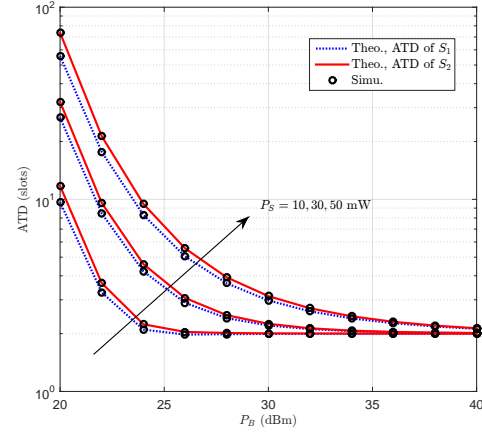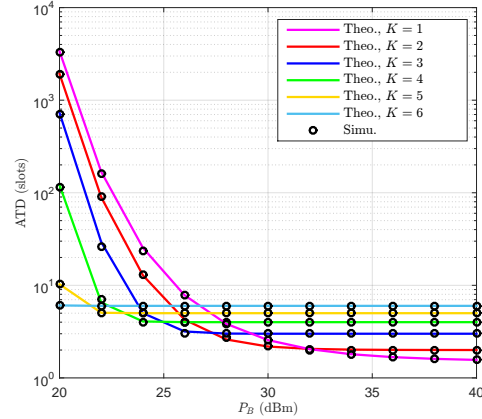
not identically distributed channels. Generally speaking, the sources that are more close to the power beacon will have lower ATD. Furthermore, we observe in both two figures that the ATD becomes about 2 time slots when P_B becomes large, which is equal to the number of the sources. Moreover, we see that the ATD rises sharply when the power beacon gets far from the sources. Furthermore, Fig. 13 depicts that the ATD for all the sources would increase when the transmit power of sources is promoted. We note that, under the given conditions, $P_S = 10, 30, 50$ mW actually corresponds to $l_S = 1, 3, 5$, respectively. As a result, by promoting P_S, on the one hand, it needs to spend much more time slots for the sources to accumulate sufficient energy, and on the other hand, the energy consumption of the IT operation would also increase.

Figs. 14 plots the ATD of S_1 versus the transmit power of the power beacon P_B with different K. It is noted that similar results can be derived for other sources. Similar with Figs. 12-13, we find that the ATD could be rather huge in the low regime of P_B. However, when the number of the sources

increase gradually, the ATD performance could be improved drastically. For example, when $P_B = 20$ dBm, the ATD will decline from about 3000 time slots when $K = 1$ to just about 6 time slots when $K = 6$. Furthermore, when P_B gets high, the ATD reduces quickly and eventually reaches a constant, which is about K. We note that the best ATD performance is also K in a network where all the sources are energy-sufficient, which is resulted from the source selection approach. All above results imply the validity to improve ATD performance by deploying more sources in the network, especially when the wireless energy is not so sufficient.

VI. CONCLUSIONS

In this paper, we presented a general Markov-based model for the PB assisted multi-source wireless-powered network with our proposed source selection transmission scheme, which captures the dynamic energy behaviors of the state transitions of the whole network. Two network operating modes, the IT mode with ZF beamforming and the non-IT mode with equal power transmision, were proposed for sustainable energy utilization and reliable data transmission. To characterize the reliability of proposed network, the EOP and COP of the network were both derived. To quantify the delay brought by the source selection transmission, the ATD was also defined and derived. All the analytical results are validated by simulation, and the results shown that the EOP, COP, and ATD can be significantly improved via increasing the number of sources deployed in the proposed network.

REFERENCES

[1] S. Tang and L. Tan, "Reward rate maximization and optimal transmission policy of EH device with temporal death in EH-WSNs," *IEEE Trans. Wireless Commun.*, vol. 16, no. 2, pp. 1157–1167, Feb., 2017.

[2] D. Sui, F. Hu, W. Zhou, M. Shao, and M. Chen, "Relay selection for radio frequency energy-harvesting wireless body area network with buffer," *IEEE Internet Things J.*, to appear, 2017.

[3] U. Raza, P. Kulkarni, and M. Sooriyabandara, "Low power wide area networks: An overview," *IEEE Commun. Surveys Tuts.*, vol. 19, no. 2, pp. 855–873, 2nd quart., 2017.

[4] D. Wu, Y. Cai, and M. Guizani, "Asynchronous flow scheduling for green ambient assisted living communications," *IEEE Communications Magazine*, vol. 53, no. 1, pp. 64–70, Jan., 2015.

[5] L. P. Qian, G. Feng, and V. C. M. Leung, "Optimal transmission policies for relay communication networks with ambient energy harvesting relays," *IEEE J. Sel. Areas Commun.*, vol. 34, no. 12, pp. 3754–3768, Dec., 2016.

[6] G. Pan, H. Lei, Y. Deng, L. Fan, J. Yang, Y. Chen, and Z. Ding, "On secrecy performance of MISO SWIPT systems with TAS and imperfect CSI," *IEEE Trans. Commun.*, vol. 64, no. 9, pp. 3831–3843, Sep., 2016.

[7] Z. Yang, Z. Ding, P. Fan, and N. Al-Dhahir, "The impact of power allocation on cooperative non-orthogonal multiple access networks with SWIPT," *IEEE Trans. Wireless Commun.*, vol. 16, no. 7, pp. 4332–4343, Jul., 2017.

[8] C. Zhong, H. A. Suraweera, G. Zheng, I. Krikidis, and Z. Zhang, "Wireless information and power transfer with full duplex relaying," *IEEE Trans. Commun.*, vol. 62, no. 10, pp. 3447–3461, Oct., 2014.

[9] Y. Zeng and R. Zhang, "Full-duplex wireless-powered relay with self-energy recycling," *IEEE Wireless Commun. Lett.*, vol. 4, no. 2, pp. 201–204, Apr., 2015.

[10] X. Zhou, R. Zhang, and C. K. Ho, "Wireless information and power transfer: Architecture design and rate-energy tradeoff," *IEEE Trans. Commun.*, vol. 61, no. 11, pp. 4754–4767, Nov., 2013.

[11] D. Wang, R. Zhang, X. Cheng, and L. Yang, "Capacity-enhancing full-duplex relay networks based on power splitting (PS-)SWIPT," *IEEE Trans. Veh. Techno.*, vol. 66, no. 6, pp. 5445–5450, Jun., 2017.

[12] X. Zhou, "Training-based SWIPT: Optimal power splitting at the receiver," *IEEE Trans. Veh. Techno.*, vol. 64, no. 9, pp. 4377–4382, Sep., 2015.

[13] K. Huang and X. Zhou, "Cutting the last wires for mobile communications by microwave power transfer," *IEEE Commun. Mag.*, vol. 53, no. 6, pp. 86–93, Jun., 2015.

[14] X. Zhou, J. Guo, S. Durrani, and M. D. Renzo, "Power beacon-assisted millimeter wave Ad Hoc networks," *IEEE Trans. Commun.*, vol. 66, no. 2, pp. 830–844, Feb., 2018.

[15] "Cota: Real wireless power," *CES 2017 Innovation Awards*, [Online]. Available: http://www.ces.tech/Events-Experiences/Innovation-Awards-Program/Honorees.aspx. and http://www.ossia.com/cota/.

[16] X. Jiang, C. Zhong, Z. Zhang, and G. Karagiannidis, "Power beacon assisted wiretap channels with jamming," *IEEE Trans. Wireless Commun.*, vol. 15, no. 12, pp. 8353–8367, Dec., 2016.

[17] Y. Ma, H. Chen, Z. Lin, Y. Li, and B. Vucetic, "Distributed and optimal resource allocation for power beacon-assisted wireless-powered communications," *IEEE Trans. Commun.*, vol. 63, no. 10, pp. 3569–3583, Oct., 2015.

[18] L. Chen, W. Wang, and C. Zhang, "Stochastic wireless powered communication networks with truncated cluster point process," *IEEE Trans. Veh. Techno.*, vol. 66, no. 12, pp. 11 286–11 294, Dec., 2017.

[19] L. Shi, L. Zhao, K. Liang, and H. H. Chen, "Wireless energy transfer enabled D2D in underlaying cellular networks," *IEEE Trans. Veh. Techno.*, vol. 67, no. 2, pp. 1845–1849, Feb., 2018.

[20] A. Salem, K. A. Hamdi, and K. M. Rabie, "Physical layer security with RF energy harvesting in AF multi-antenna relaying networks," *IEEE Trans. Commun.*, vol. 64, no. 7, pp. 3025–3038, Jul., 2016.

[21] C. Pielli, C. Stefanovic, P. Popovski, and M. Zorzi, "Joint compression, channel coding and retransmission for data fidelity with energy harvesting," *IEEE Trans. Commun.*, to appear, 2017.

[22] Y. Bi and H. Chen, "Accumulate and jam: Towards secure communication via a wireless-powered full-duplex jammer," *IEEE J. Sel. Topics Signal Process.*, vol. 10, no. 8, pp. 1538–1550, Dec., 2016.

[23] H. Liu, K. J. Kim, K. S. Kwak, and H. V. Poor, "Power splitting-based SWIPT with decode-and-forward full-duplex relaying," *IEEE Trans. Wireless Commun.*, vol. 15, no. 11, pp. 7561–7577, Nov., 2016.

[24] ——, "QoS-constrained relay control for full-duplex relaying with SWIPT," *IEEE Trans. Wireless Commun.*, vol. 16, no. 5, pp. 2936–2949, May, 2017.

[25] I. Ahmed, K. T. Phan, and T. Le-Ngoc, "Stochastic user scheduling and power control for energy harvesting networks with statistical delay provisioning," in *2015 IEEE 26th Annual International Symposium on Personal, Indoor, and Mobile Radio Communications (PIMRC)*, Hong Kong, China, 2015.

[26] Q. Yao, T. Q. S. Quek, A. Huang, and H. Shan, "Joint downlink and uplink energy minimization in WET-enabled networks," *IEEE Trans. Wireless Commun.*, vol. 16, no. 10, pp. 6751–6765, Oct., 2017.

[27] I. Krikidis, S. Timotheou, S. Nikolaou, G. Zheng, D. W. K. Ng, and R. Schober, "Simultaneous wireless information and power transfer in modern communication systems," *IEEE Commun. Mag.*, vol. 52, no. 11, pp. 104–110, Nov., 2014.

[28] J. Zhang, C. Yuen, C. K. Wen, S. Jin, K. K. Wong, and H. Zhu, "Large system secrecy rate analysis for SWIPT MIMO wiretap channels," *IEEE Trans. Inf. Forensics Security*, vol. 11, no. 1, Jan., 2016.

[29] K. Hosseini, W. Yu, and R. S. Adve, "Large-scale MIMO versus network MIMO for multicell interference mitigation," *IEEE J. Sel. Topics Signal Process.*, vol. 8, no. 5, pp. 930–941, Oct., 2014.

[30] A. Bletsas, A. Khisti, D. P. Reed, and A. Lippman, "A simple cooperative diversity method based on network path selection," *IEEE J. Sel. Areas Commun.*, vol. 24, no. 3, pp. 659–672, Mar., 2006.

[31] X. Tang, Y. Cai, Y. Huang, T. Q. Duong, W. Yang, and W. Yang, "Secrecy outage analysis of buffer-aided cooperative MIMO relaying systems," *IEEE Trans. Veh. Techno.*, to appear, 2017.

[32] Z. Ding, Z. Zhao, M. Peng, and H. V. Poor, "On the spectral efficiency and security enhancements of NOMA assisted multicast-unicast streaming," *IEEE Trans. Commun.*, vol. 65, no. 7, pp. 3151–3163, Jul., 2017.

[33] A. Yilmaz, F. Yilmaz, M. S. Alouini, and O. Kucur, "On the performance of transmit antenna selection based on shadowing side information," *IEEE Trans. Veh. Techno.*, vol. 62, no. 1, pp. 454–460, Jan., 2013.

[34] I. Krikidis, T. Charalambous, and J. S. Thompson, "Buffer-aided relay selection for cooperative diversity systems without delay constraints," *IEEE Trans. Wireless Commun.*, vol. 11, no. 5, pp. 1957–1967, May, 2012.

Xuanxuan Tang received his B.S. degree in Communication Engineering from the College of Communications Engineering, PLA University of Science and Technology, Nanjing, China, in 2014. He is currently pursuing toward the Ph.D. degree in Information and Communications Engineering at the College of Communications Engineering, Army Engineering University of PLA, Nanjing, China. His current research interest includes cooperative communications, wireless sensor networks, Internet of Things, physical layer security, energy harvesting, full-duplex, and cognitive radio systems.

Yansha Deng (S'13-M'17) is currently a Lecturer (Assistant Professor) in department of Informatics, King's College London, U. K. She received the Ph.D. degree in Electrical Engineering from the Queen Mary University of London, UK in 2015. From 2015 to 2017, she was a Post-Doctoral Research Fellow with King's College London, UK. Her research interests include molecular communication, internet of things, and 5G wireless networks. She was a recipient of the Best Paper Awards from ICC 2016 and Globecom 2017. She is currently an Editor of IEEE Transactions on Communications and IEEE Communication Letters. She has also served as TPC member for many IEEE conferences, such as IEEE GLOBECOM and ICC.

Yueming Cai (M'05-SM'12) received his B.S. degree in Physics from Xiamen University, Xiamen, China in 1982, the M.S. degree in Micro-electronics Engineering and the Ph.D. degree in Communications and Information Systems both from Southeast University, Nanjing, China in 1988 and 1996, respectively. His current research interests include MIMO systems, OFDM systems, signal processing in communications, cooperative communications and wireless sensor networks.

Wendong Yang received the B.S. degree in Communications Engineering and the Ph.D. degree in Communications and Information Systems both from College of Communications Engineering, PLA University of Science and Technology, Nanjing, China in 2004 and 2009 respectively. His current research interest includes MIMO systems, OFDM systems, cooperative communications and cognitive radio.

Arumugam Nallanathan (S'97-M'00-SM'05-F'17) is Professor of Wireless Communications and Head of the Communication Systems Research (CSR) group in the School of Electronic Engineering and Computer Science at Queen Mary University of London since September 2017. He was with the Department of Informatics at Kings College London from December 2007 to August 2017, where he was Professor of Wireless Communications from April 2013 to August 2017 and a Visiting Professor from September 2017. He was an Assistant Professor in the Department of Electrical and Computer Engineering, National University of Singapore from August 2000 to December 2007. His research interests include 5G Wireless Networks, Internet of Things (IoT) and Molecular Communications. He published nearly 400 technical papers in scientific journals and international conferences. He is a co-recipient of the Best Paper Awards presented at the IEEE International Conference on Communications 2016 (ICC2016) , IEEE Global Communications Conference 2017 (GLOBECOM2017) and IEEE Vehicular Technology Conference 2018 (VTC2018). He is an IEEE Distinguished Lecturer. He has been selected as a Web of Science Highly Cited Researcher in 2016. He is an Editor for IEEE Transactions on Communications. He was an Editor for IEEE Transactions on Wireless Communications (2006-2011), IEEE Transactions on Vehicular Technology (2006-2017), IEEE Wireless Communications Letters and IEEE Signal Processing Letters. He served as the Chair for the Signal Processing and Communication Electronics Technical Committee of IEEE Communications Society and Technical Program Chair and member of Technical Program Committees in numerous IEEE conferences. He received the IEEE Communications Society SPCE outstanding service award 2012 and IEEE Communications Society RCC outstanding service award 2014.